Electronic Supplementary Material (ESI) for Dalton Transactions

Supplementary Information

Synthesis and complexes of an N_4 Schiff-base macrocycle derived from 2,2'-iminobisbenzaldehyde

Rajni Sanyal, Scott A. Cameron and Sally Brooker*[a]

[a] *Department of Chemistry and MacDiarmid Institute for Advanced Materials and Nanotechnology, University of Otago, PO Box 56, Dunedin 9054, New Zealand. Fax: +64 3 479 7906. Email: sbrooker@chemistry.otago.ac.nz*

Figure S1. ^{1}H NMR and ^{13}C NMR Spectra of HL in $CDCl_3$

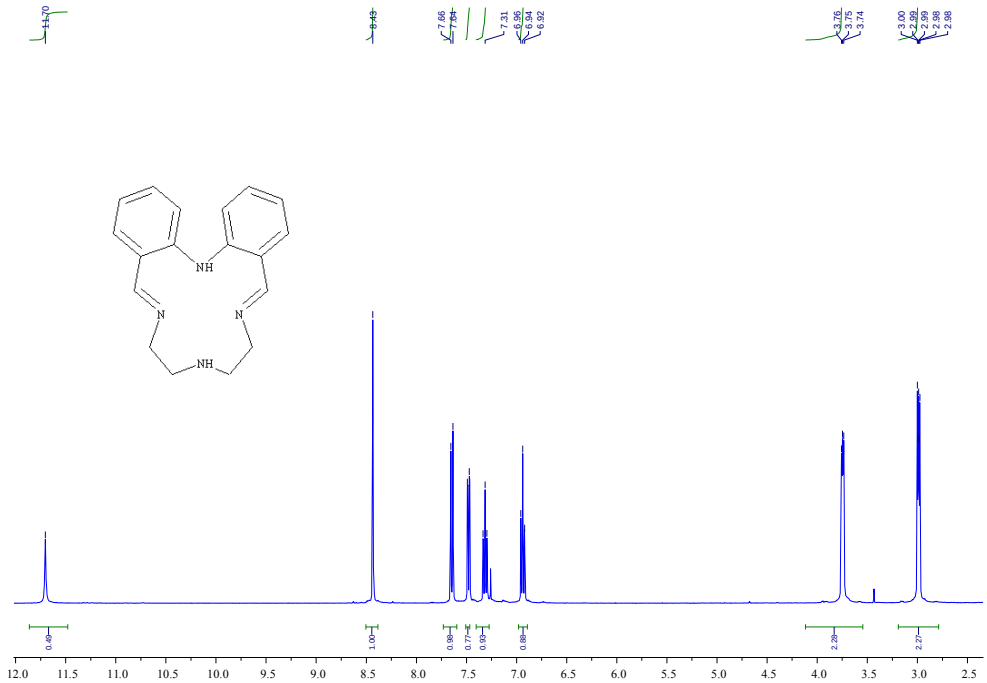

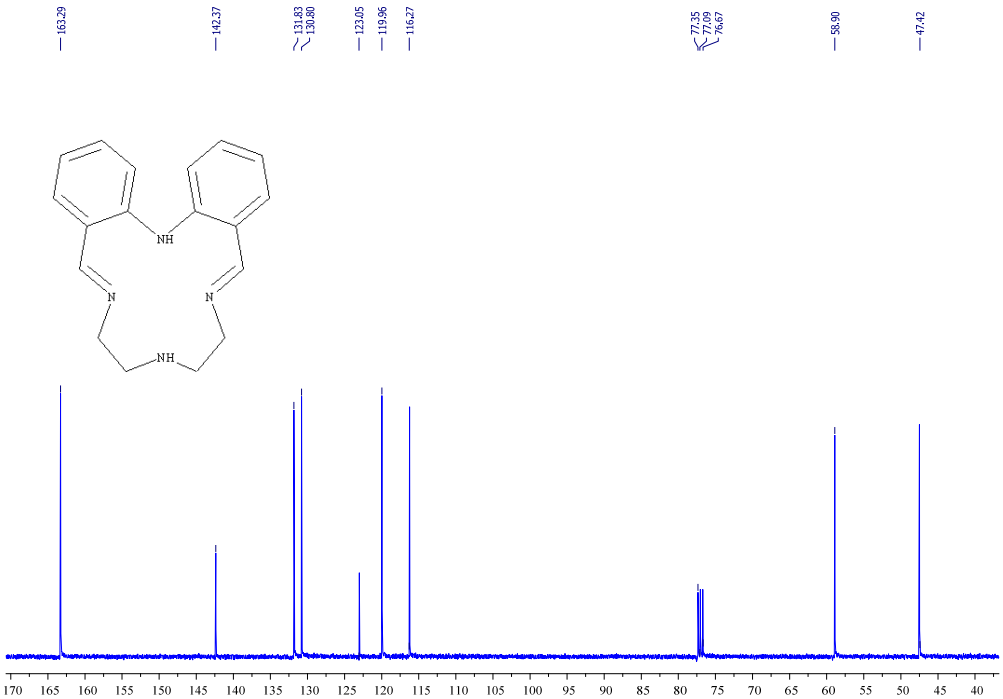

Figure S2. ^{1}H NMR and ^{13}C NMR Spectra of [ZnL(py)](BF$_4$) **2** **(**CD$_3$)$_2$CO

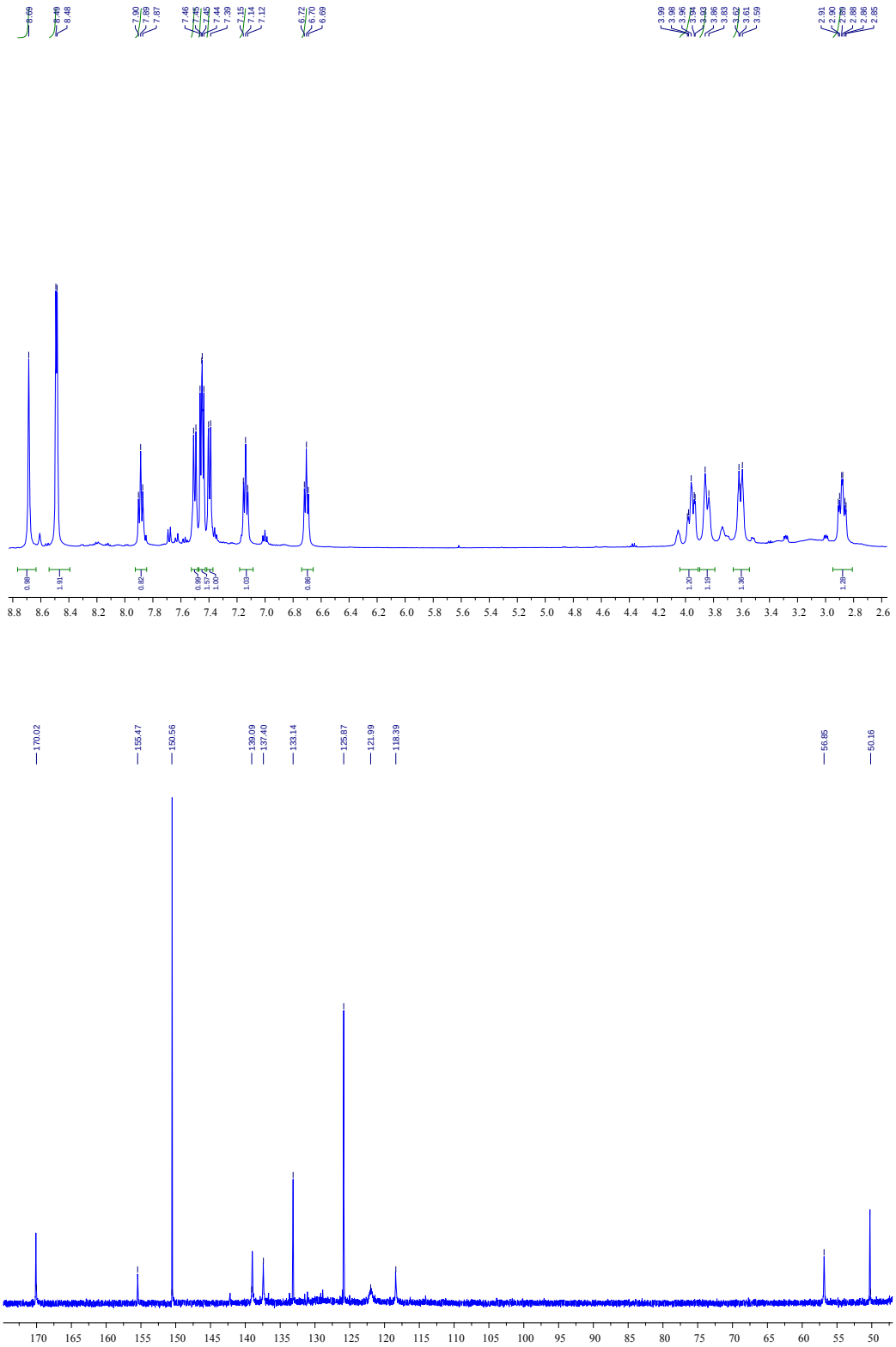

Figure S3. ^{1}H NMR and ^{13}C NMR Spectra of $[NiL](BF_4)\bullet H_2O$ **4** in CD_3CN

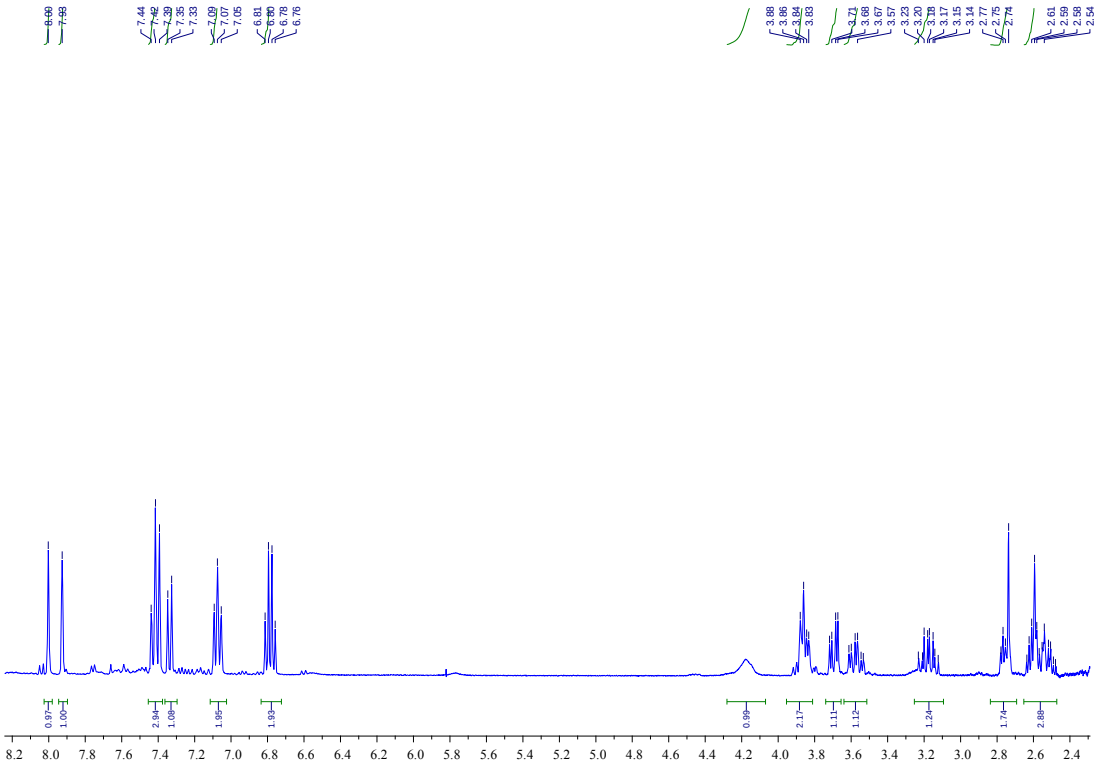

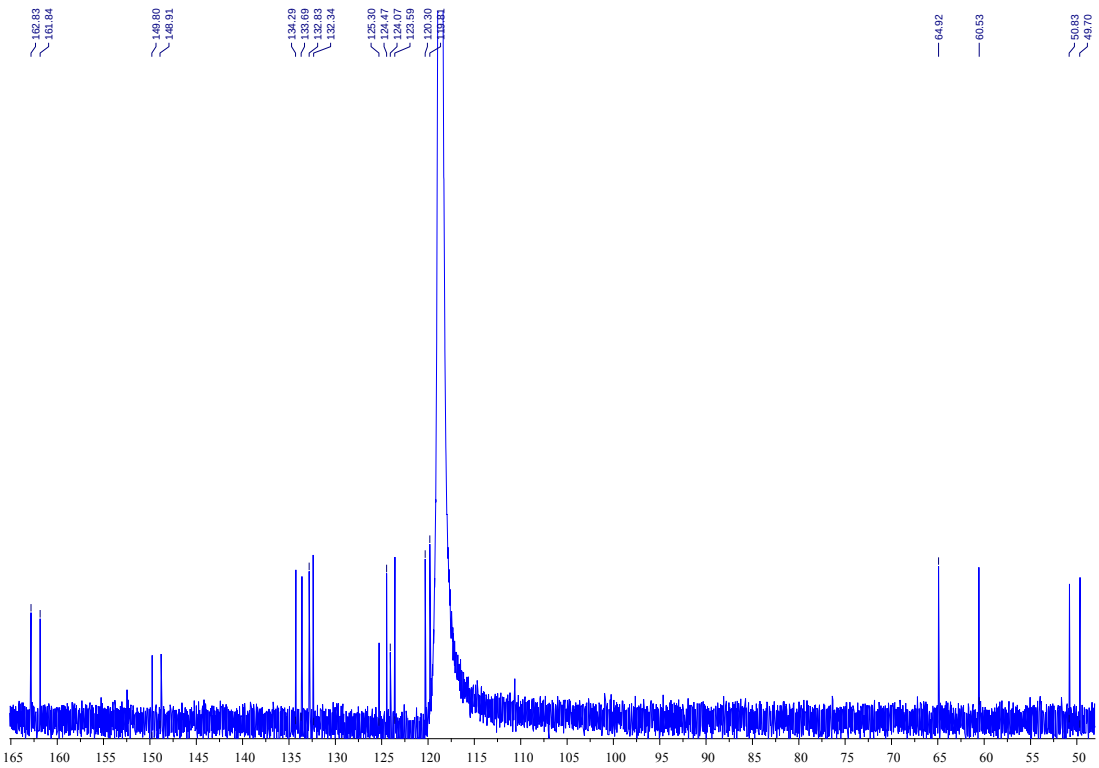

Figure S4. ^{1}H NMR and ^{13}C NMR Spectra of $[CoL(NCS)_2]$•0.3py **7** in CD_3CN

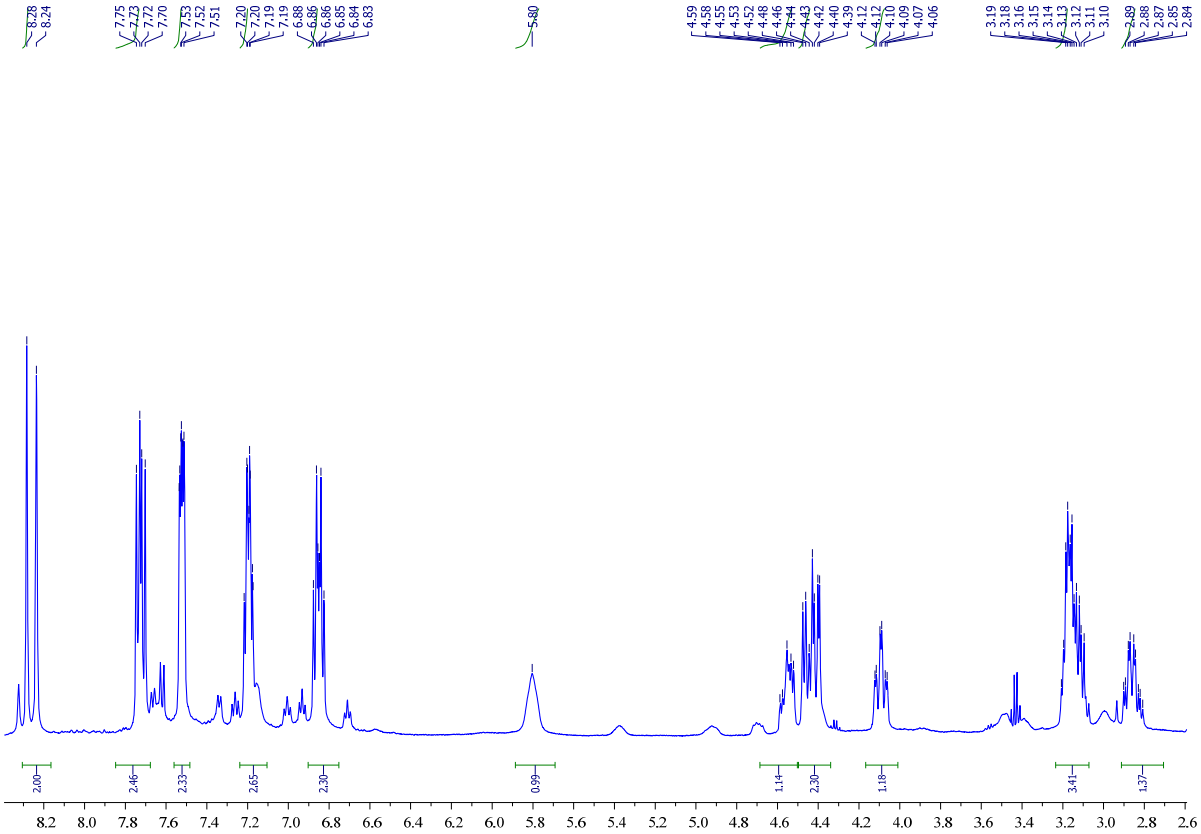

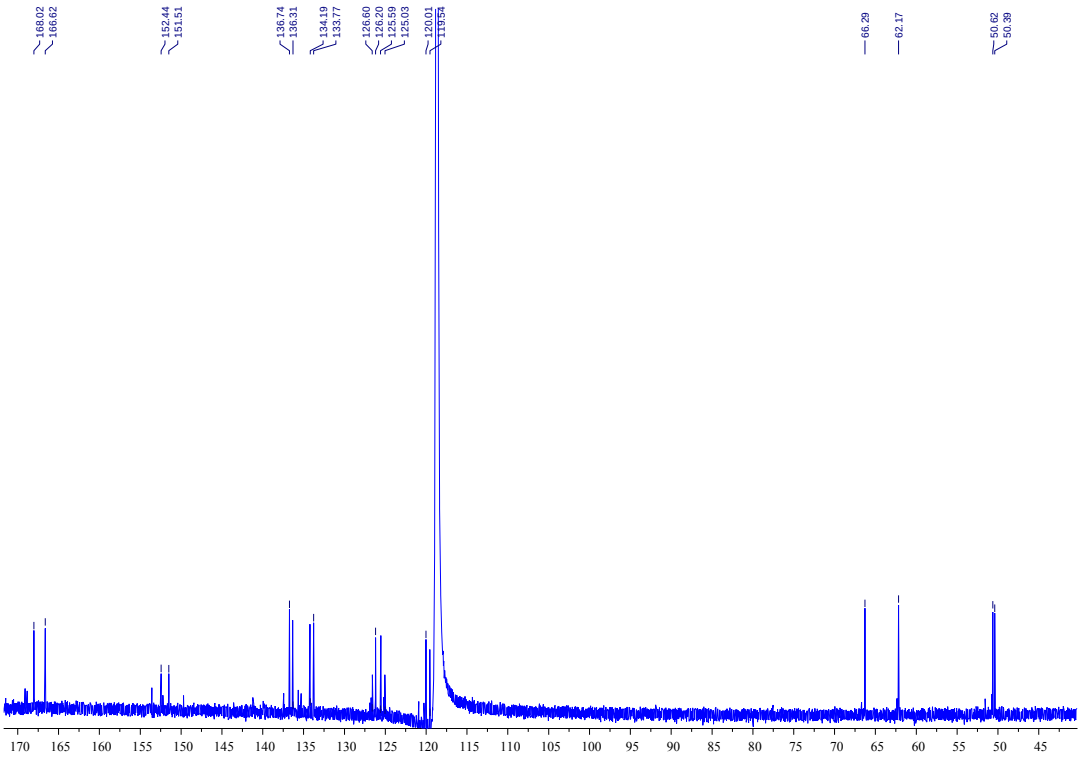

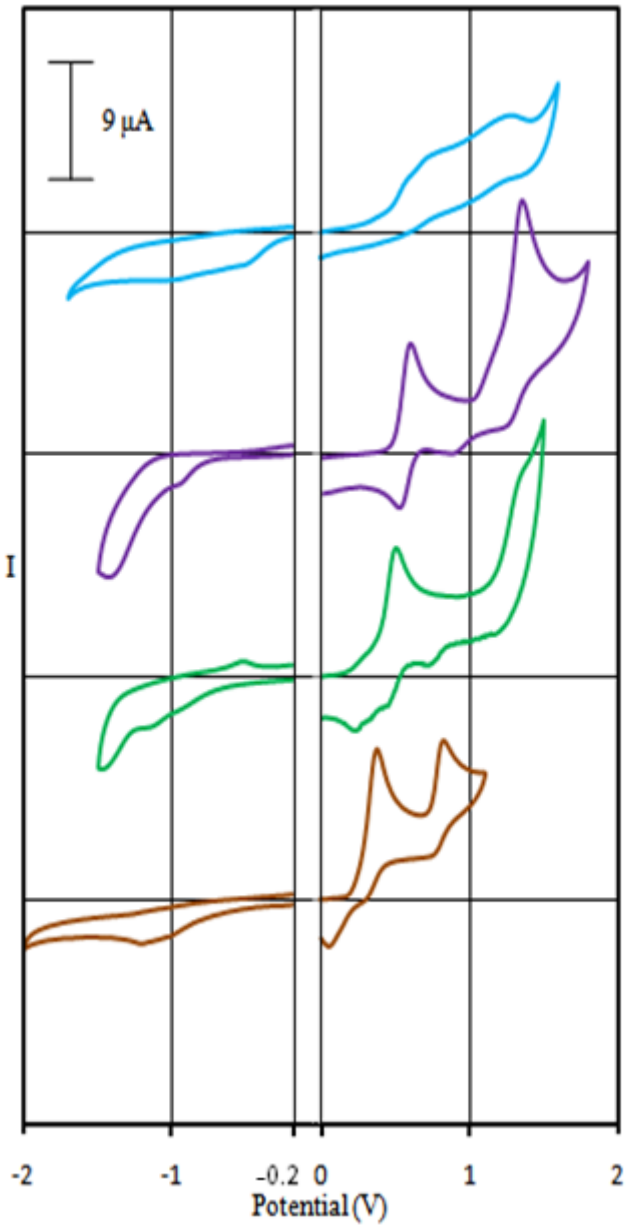

Figure S5. Cyclic voltammograms of complexes ***before*** conducting controlled potentiostatic coulometry experiment over the potential range of interest for, from bottom to top: $[Zn^{II}L(py)](BF_4)$ **2** (brown line), $[Cu^{II}L](BF_4)\bullet H_2O$ **3** (green line), $[Ni^{II}L](BF_4)\bullet H_2O$ **4** (purple line) and $[Co^{II}L](BF_4)\bullet H_2O$ **5** (blue line) as 1 mmol L^{-1} solutions in MeCN (100 $mV.s^{-1}$, 0.1 $mol.L^{-1}$ NBu_4PF_6, platinum electrode, versus 0.01 $mol.L^{-1}$ $AgNO_3/Ag$).

Electrochemical study of [ZnLPy](BF_4) in MeCN

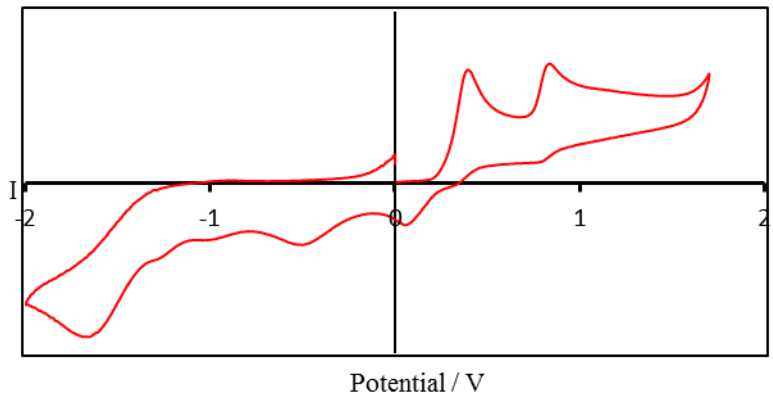

Figure S6. Cyclic voltammogram of [ZnL(py)](BF_4) **before** carrying out a controlled potential coulometry experiment at +0.48 V as 1mmol L^{-1} solutions in MeCN (200 $mV.s^{-1}$, 0.1 $mol.L^{-1}$ NEt_4PF_6, platinum electrode, versus 0.01 $mol.L^{-1}$ $AgNO_3$-Ag).

1. *First bulk electrolysis experiment, at +0.48 V*

Mass of [ZnLPy](BF_4) used = 5.2346 mg

Concentration of [ZnLPy](BF_4) = $\frac{0.0052346\ g}{0.010\ L \times 522.6607\ g\ mol^{-1}}$ = 1.002 x 10^{-5} mol L^{-1}

The expected number of electrons to be transferred provided that this particular process was a one electron process was calculated to be 0.97 coulombs. This was calculated as follows.

No. of moles of [ZnLPy](BF_4) = Concentration of [ZnLPy](BF_4) x Volume
= 0.001002 Mol L^{-1} x 0.010 L
= 1.002 x 10^{-5} mol

No. of electrons transferred = n_e x No. of moles of [ZnLPy](BF_4) x Faraday's constant
= 1 x 1.002 x 10^{-5} mol x 96500 C mol^{-1}
= 0.967 C if one electron process

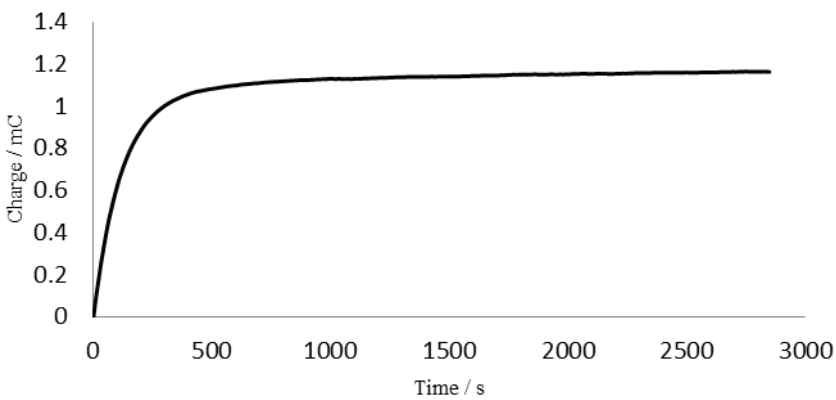

Figure S7. Controlled potentiostatic coulometry experiment conducted at +0.48 V led to 1.16 coulombs of electrons transferred which corresponds to 1.2 electron equivalents per complex.

Second run at +0.41 V

A controlled potentiostatic coulometry experiment was also carried out, on a fresh sample, at +0.41 V, about 60 mV less than the previous potential used.

Mass of $[ZnLPy](BF_4)$ used = 5.2305 mg

Concentration of $[ZnLPy](BF_4)$ = $\frac{0.0052305\ g}{0.010\ L \times 522.6607\ g\ mol^{-1}}$ = 1.001×10^{-5} mol L^{-1}

No. of moles of $[ZnLPy](BF_4)$ = Concentration of $[ZnLPy](BF_4)$ x Volume
= 0.001001 Mol L^{-1} x 0.010 L
= 1.001×10^{-5} mol

No. of electrons transferred = n_e x No. of moles of $[ZnLPy](BF_4)$ x Faraday's constant
= 1 x 1.001×10^{-5} mol x 96500 C mol^{-1}
= 0.966 C

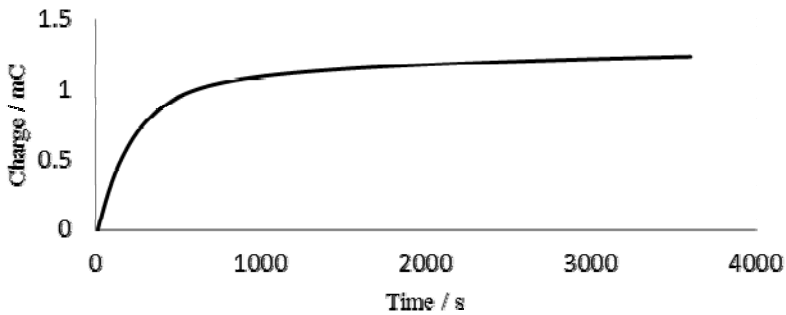

Figure S8. Controlled potentiostatic coulometry experiment conducted at +0.41 V led to 1.2 coulombs of electrons transferred which corresponds to 1.2 electron equivalents per complex.

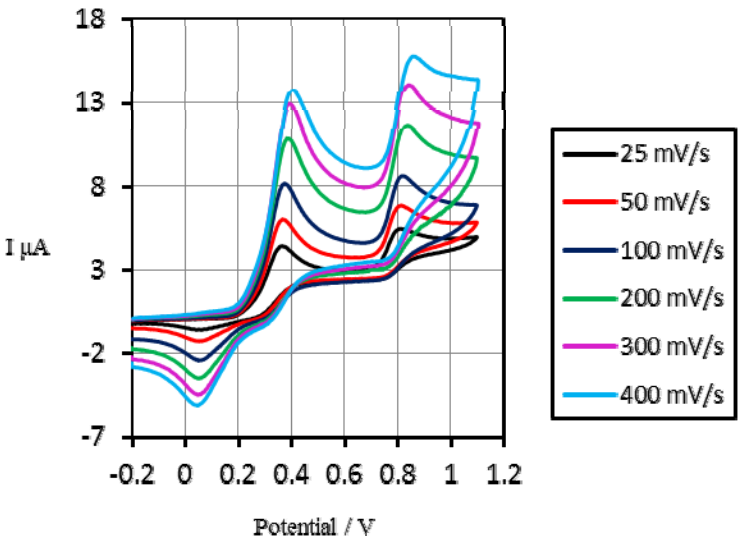

Figure S9. Cyclic voltammogram of $[ZnL(py)](BF_4)$ (oxidation process) at different scan rates ($mV.s^{-1}$) **before** conducting a controlled coulometry experiment.

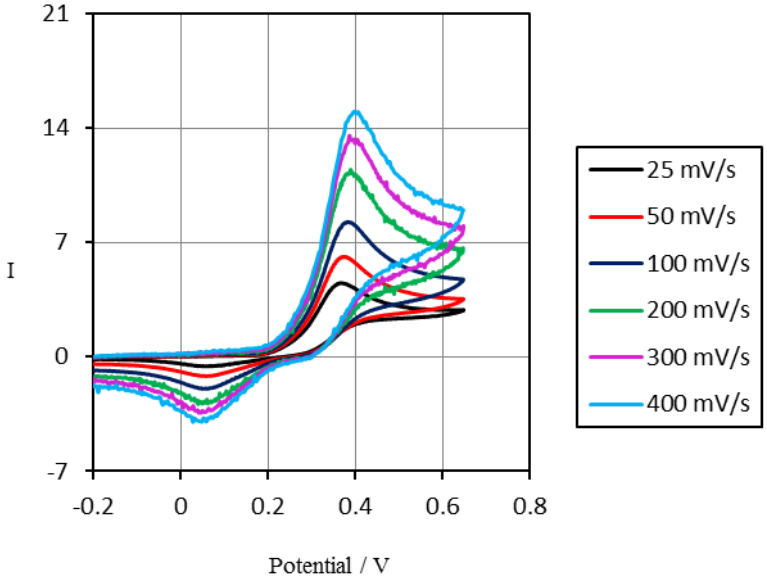

Figure S10. Cyclic voltammogram of [ZnL(py)](BF_4) (oxidation process) at different scan rates ($mV.s^{-1}$) **before** conducting a controlled coulometry experiment.

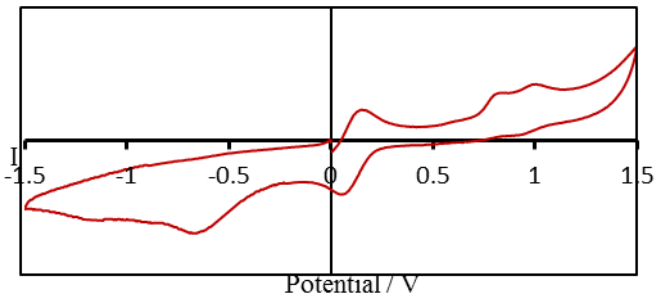

Figure S11. Cyclic voltammogram of [ZnL(py)](BF_4) **after** carrying out a controlled potential coulometry experiment at 0.47 V as 1 $mmol.L^{-1}$ solutions in MeCN (200 $mV.s^{-1}$, 0.1 $mol.L^{-1}$ NEt_4PF_6, platinum electrode, versus 0.01 $mol.L^{-1}$ $AgNO_3$-Ag).

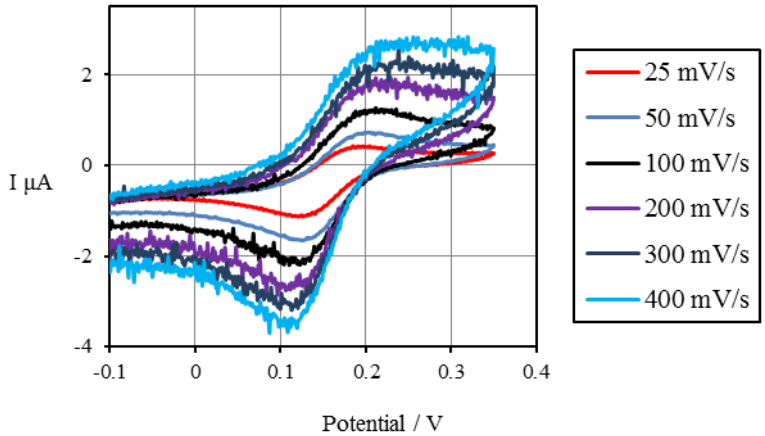

Figure S12. Cyclic voltammogram of [ZnL(py)](BF_4) (oxidation process) at different scan rates (mVs^{-1}) **after** conducting a controlled coulometry experiment.

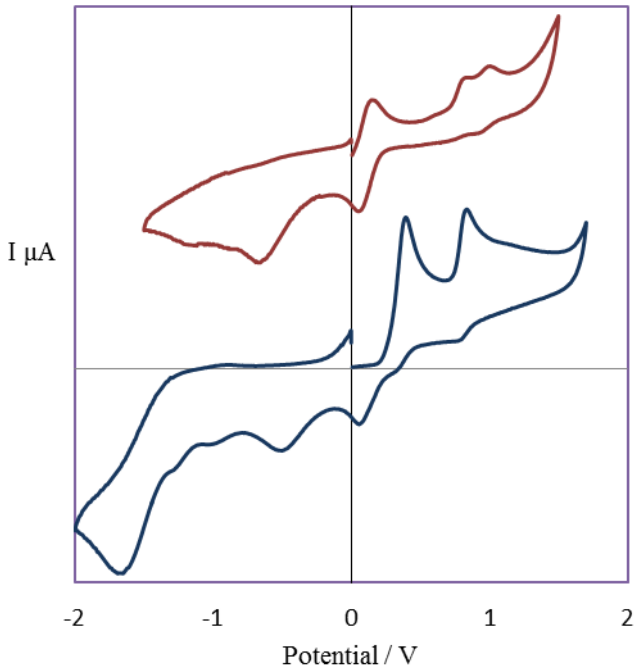

Figure S13. Cyclic voltammogram, from the bottom of [ZnLPy](BF_4) **before** (blue) and **after** (red) carrying out a controlled potential coulometry experiment at 0.47 V as 1mmol L^{-1} solutions in MeCN (200 mV.s^{-1}, 0.1 M NEt_4PF_6, platinum electrode, versus 0.01 M $AgNO_3$/Ag).

Electrochemical study of $[CuL](BF_4)\bullet H_2O$ in MeCN

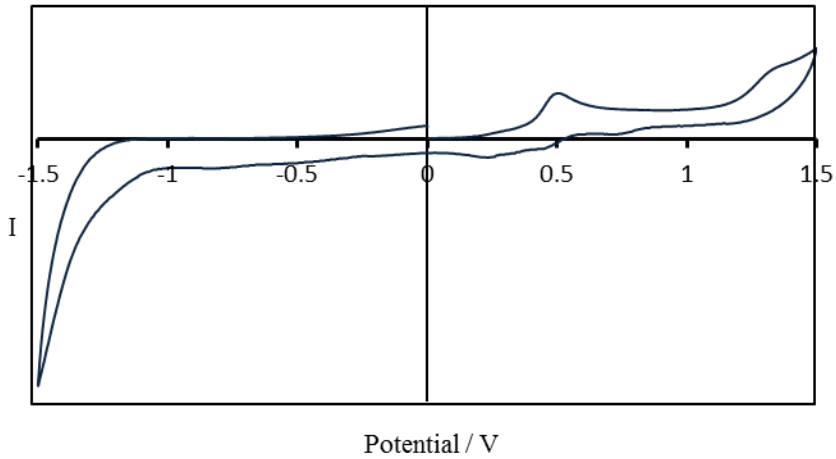

Figure S14. Cyclic voltammogram of $[CuL](BF_4)\bullet H_2O$ **before** carrying out a controlled potential coulometry experiment at +0.61 V as 1mmol L^{-1} solutions in MeCN (200 $mV.s^{-1}$, 0.1 M NEt_4PF_6, platinum electrode, versus 0.01 M $AgNO_3$-Ag).

Mass of $[CuL](BF_4)\bullet H_2O$ used = 5.2346 mg

Concentration of $[CuL](BF_4)\bullet H_2O$ = $\frac{0.0052346\ g}{0.010\ L \times 522.6607\ g\ mol^{-1}}$ = 1.002 x 10^{-5} mol L^{-1}

The expected number of electrons to be transferred provided that this particular process was a one electron process was calculated to be 0.97 coulombs. This was calculated from the following equation.

No. of moles of $[CuL](BF_4)\bullet H_2O$ = Concentration of $[CuL](BF_4)\bullet H_2O$ x Volume
= 0.00100 Mol L^{-1} x 0.010 L
= 0.00001 mol

No. of electrons transferred = n_e x No. of moles of $[CuL](BF_4)\bullet H_2O$ x Faraday's constant
= 1 x 0.00001 mol x 96500 C mol^{-1}
= 0.966 C if one electron process

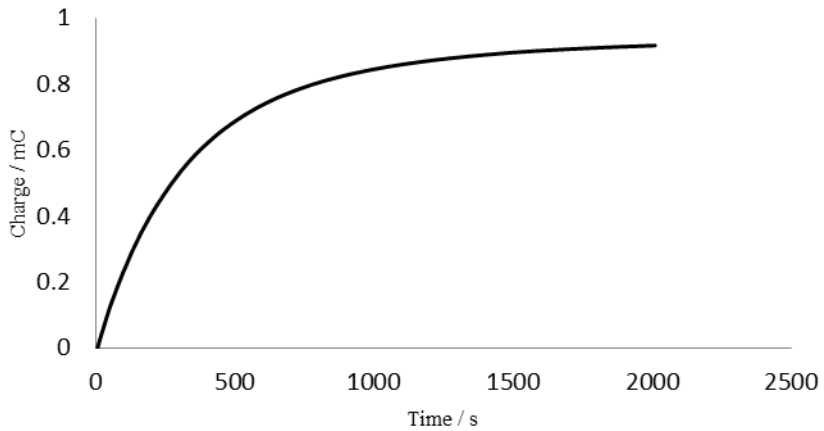

Figure S15. Controlled potentiostatic coulometry experiment conducted at +0.61 V led to 0.92 coulombs of electrons transferred which corresponds to 0.95 electron equivalents per complex

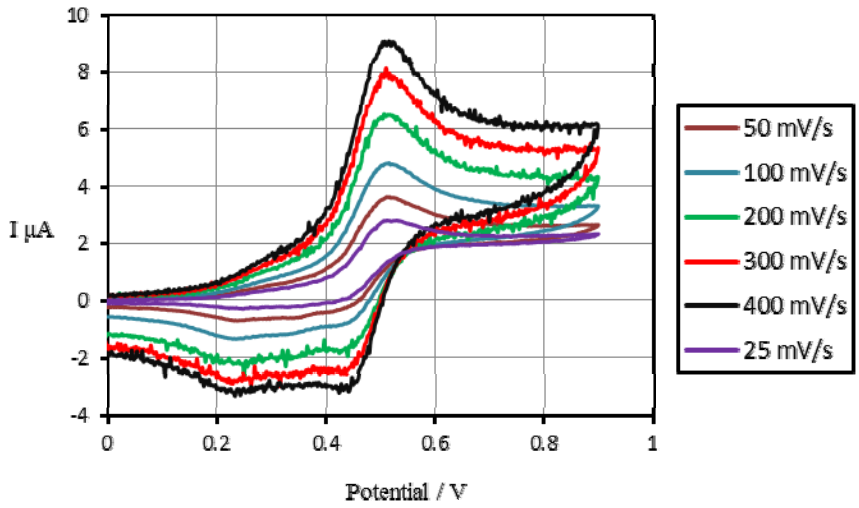

Figure S16. Cyclic voltammogram of $[CuL](BF_4)\bullet H_2O$ (oxidation process) at different scan rates ($mV.s^{-1}$) **before** conducting a controlled coulometry experiment.

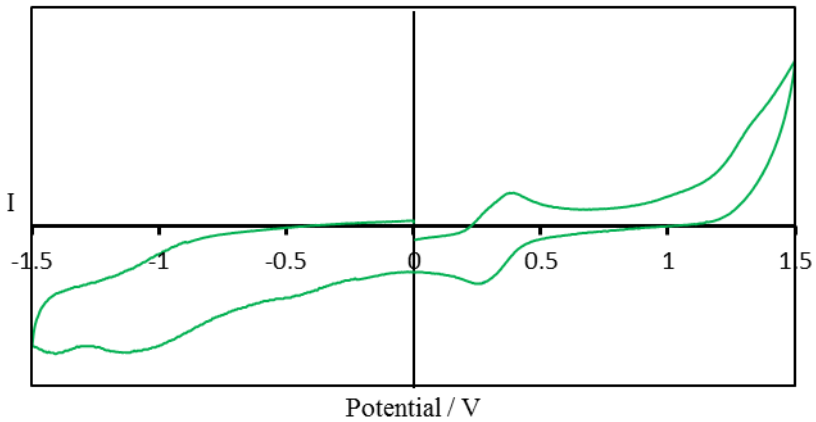

Figure S17. Cyclic voltammogram of $[CuL](BF_4)\bullet H_2O$ **after** carrying out a controlled potential coulometry experiment at +0.61 V as 1 $mmol.L^{-1}$ solutions in MeCN (200 $mV.s^{-1}$, 0.1 $mol.L^{-1}$ NEt_4PF_6, platinum electrode, versus 0.01 $mol.L^{-1}$ $AgNO_3$-Ag).

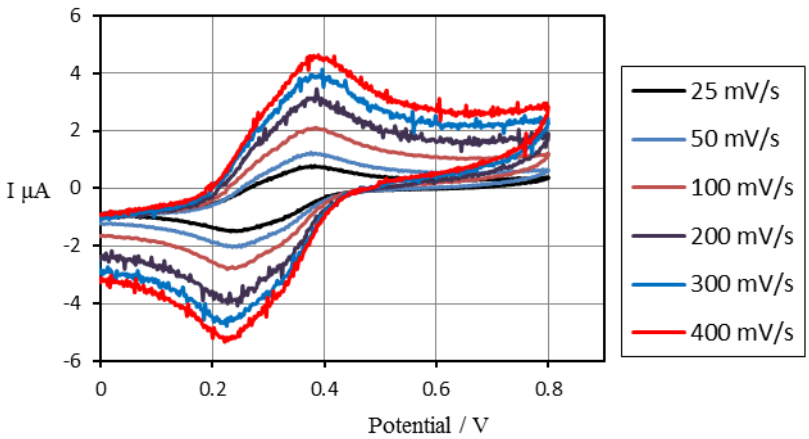

Figure S18. Cyclic voltammogram of $[CuL](BF_4)\bullet H_2O$ (oxidation process) at different scan rates ($mV.s^{-1}$) **after** conducting a controlled coulometry experiment.

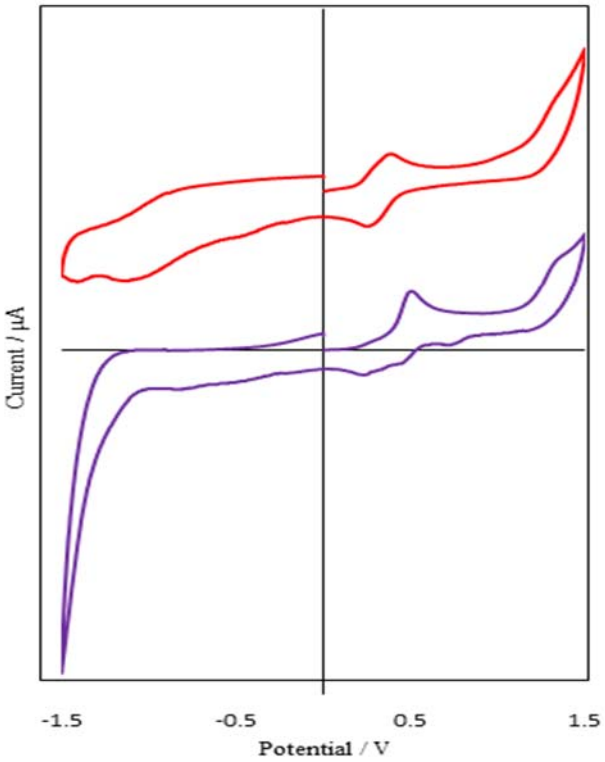

Figure S19. Cyclic voltammogram, from the bottom of $[CuL](BF_4)\bullet H_2O$ **before** (purple) and **after** (red) carrying out a controlled potential coulometry experiment at 0.61 V as 1 mmol.L^{-1} solutions in MeCN (200 mV.s^{-1}, 0.1 mol.L^{-1} NEt_4PF_6, platinum electrode, versus 0.01 mol.L^{-1} $AgNO_3$/Ag).

Electrochemical study of $[NiL](BF_4)\bullet H_2O$ in MeCN

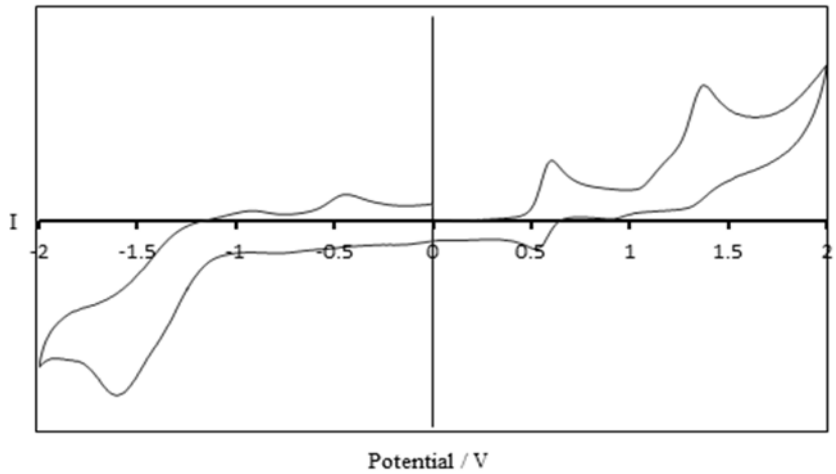

Figure S20. Cyclic voltammogram of $[NiL](BF_4)\bullet H_2O$ **before** carrying out a controlled potential coulometry experiment at +0.71 V as 1 mmol.L^{-1} solutions in MeCN (200 mV.s^{-1}, 0.1 mol.L^{-1} NEt_4PF_6, platinum electrode, versus 0.01 mol.L^{-1} $AgNO_3$-Ag).

1. First run at +0.71 V

Mass of $[NiL](BF_4)\bullet H_2O$ used = 4.500 mg

Concentration of $[NiL](BF_4)\bullet H_2O$ = $\frac{0.004500\ g}{0.010\ L \times 436.8698\ g\ mol^{-1}}$ = 1.030 x 10^{-3} mol L^{-1}

The expected number of electrons to be transferred provided that this particular process was a one electron process was 0.97 coulombs. This was calculated as follows.

No. of moles of $[NiL](BF_4)\bullet H_2O$ = Concentration of $[NiL](BF_4)\bullet H_2O$ x Volume
= 0.00103 mol L^{-1} x 0.010 L
= 0.00001 mol

No. of electrons transferred = n_e x No. of moles of $[NiL](BF_4)\bullet H_2O$ x Faraday's constant
= 1 x 0.00001 mol x 96500 C mol^{-1}
= 0.966 C if one electron process

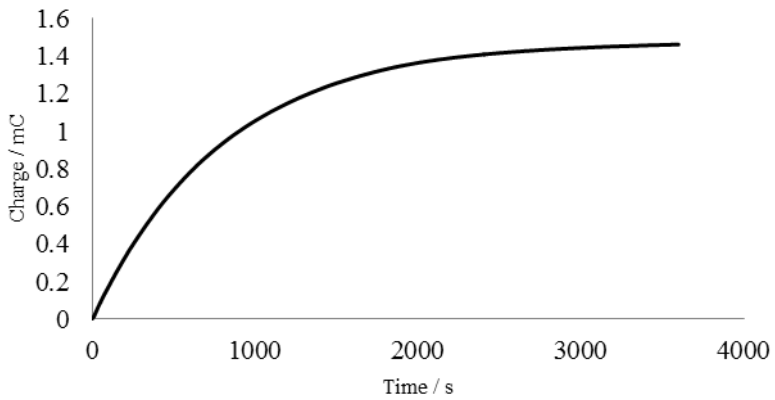

Figure S21. Controlled potentiostatic coulometry experiment conducted at +0.71 V led to 1.50 coulombs of electrons transferred which corresponds to 1.6 electron equivalents per complex.

Second run at +0.65 V

A controlled potentiostatic coulometry experiment was also carried out on a fresh sample at +0.65 V, about 60 mV less than the previous potential used.

Mass of $[NiL](BF_4)\bullet H_2O$ used = 4.5417 mg

Concentration of $[NiL](BF_4)\bullet H_2O$ = $\frac{0.0045417\ g}{0.010\ L \times 436.8698\ g\ mol^{-1}}$ = 1.046 x 10^{-3} mol L^{-1}

No. of moles of $[NiL](BF_4)\bullet H_2O$ = Concentration of $[NiL](BF_4)\bullet H_2O$ x Volume
= 0.001046 Mol L^{-1} x 0.010 L
= 1.05 x 10^{-5} mol

No. of electrons transferred = n_e x No. of moles of $[NiL](BF_4)\bullet H_2O$ x Faraday's constant
= 1 x 1.05 $\times 10^{-5}$ mol x 96500 C mol^{-1}
= 1.013 C if one electron process

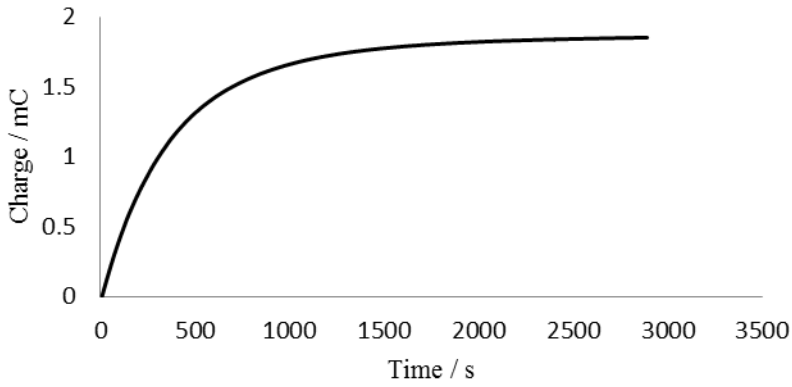

Figure S22. Controlled potentiostatic coulometry experiment conducted at +0.65 V led to 1.85 coulombs of electrons transferred which corresponds to 1.8 electron equivalents per complex.

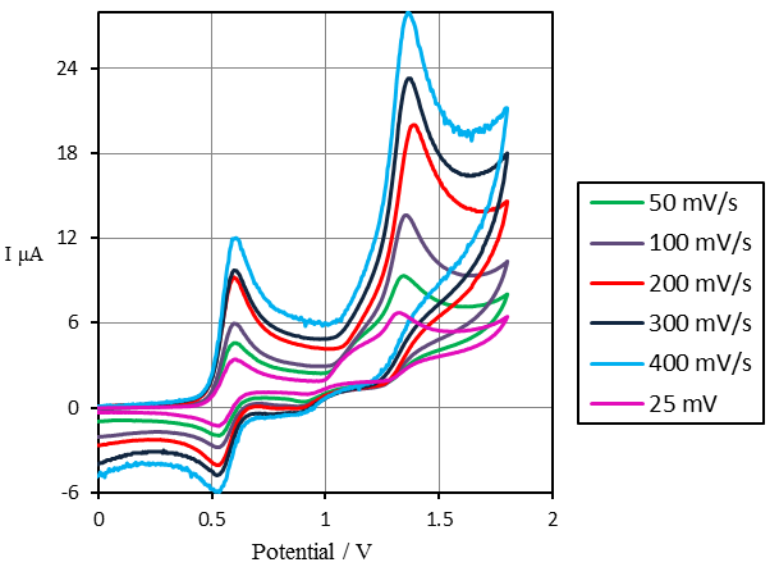

Figure S23. Cyclic voltammogram of $[NiL](BF_4)\bullet H_2O$ (oxidation process) at different scan rates ($mV.s^{-1}$) **before** conducting a controlled coulometry experiment.

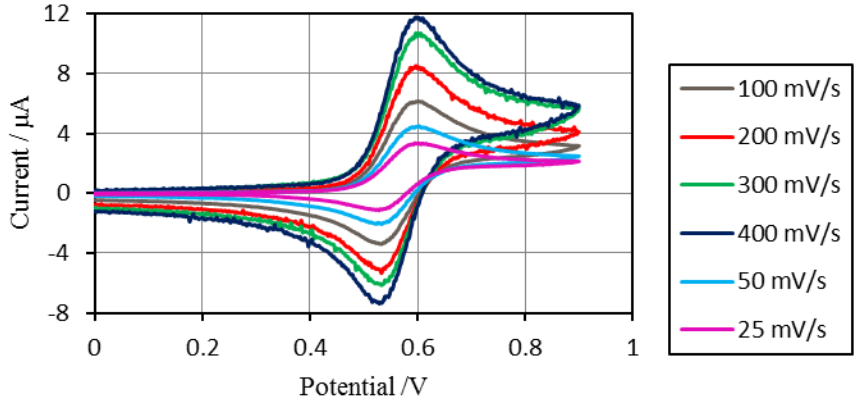

Figure S24. Cyclic voltammogram of $[NiL](BF_4)\bullet H_2O$ (oxidation process) at different scan rates ($mV.s^{-1}$) **before** conducting a controlled coulometry experiment.

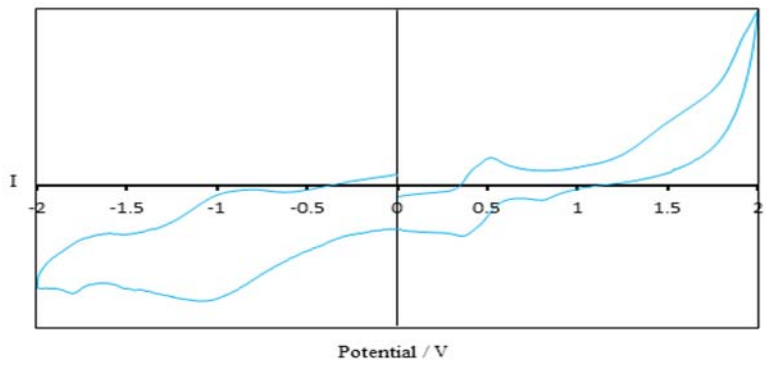

Figure S25. Cyclic voltammogram of $[NiL](BF_4)\bullet H_2O$ **after** carrying out a controlled potential coulometry experiment at +0.71 V as 1 $mmol.L^{-1}$ solutions in MeCN (200 $mV.s^{-1}$, 0.1 $mol.L^{-1}$ NEt_4PF_6, platinum electrode, versus 0.01 $mol.L^{-1}$ $AgNO_3$-Ag).

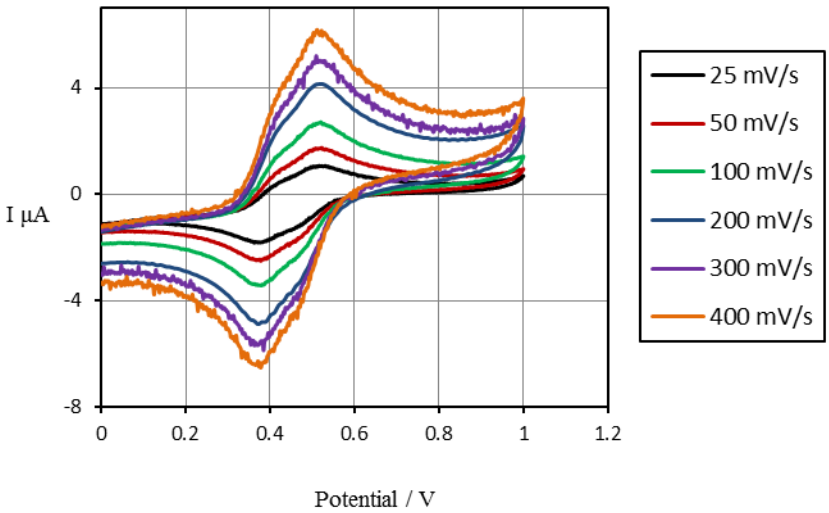

Figure S26. Cyclic voltammogram of $[NiL](BF_4)\bullet H_2O$ (oxidation process) at different scan rates (mVs^{-1}) **after** conducting a controlled coulometry experiment.

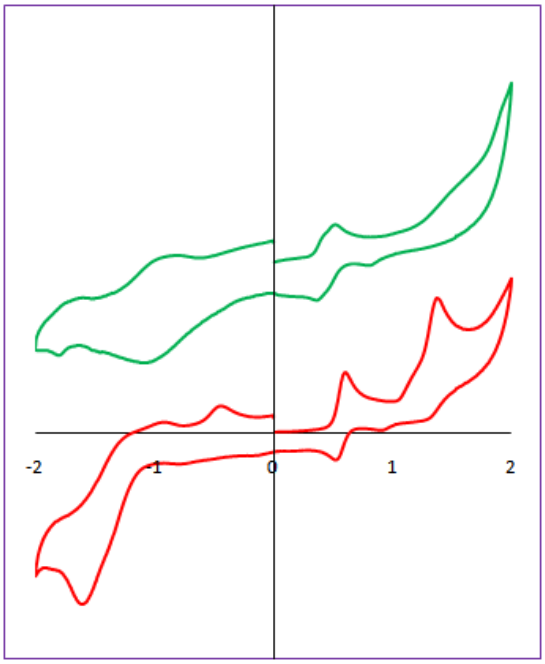

Figure S27. Cyclic voltammogram, from the bottom of $[NiL](BF_4)\bullet H_2O$ **before** (red) and after (green) carrying out a controlled potential coulometry experiment at 0.61 V as 1 $mmol.L^{-1}$ solutions in MeCN (200 $mV.s^{-1}$, 0.1 $mol.L^{-1}$ NEt_4PF_6, platinum electrode, versus 0.01 $mol.L^{-1}$ $AgNO_3$-Ag).

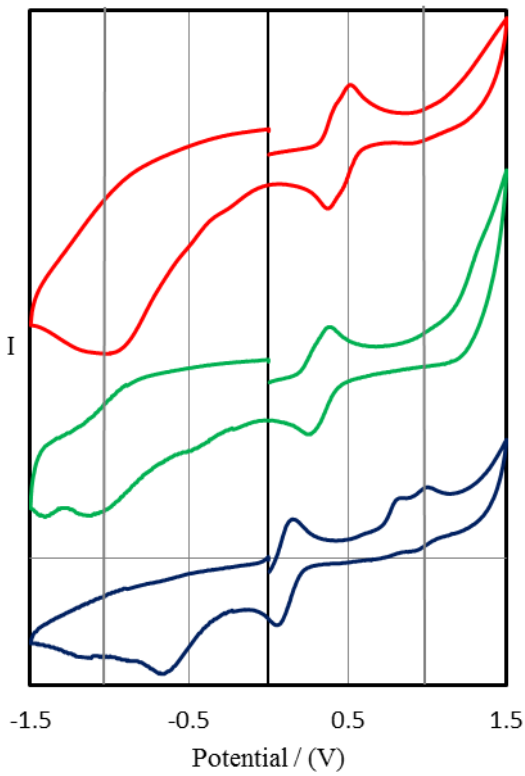

Figure S28. Cyclic voltammograms of the three BF_4 complexes from the bottom $[ZnL(py)](BF_4)$ **2** (blue), $[CuL](BF_4)\bullet H_2O$ **3** (green) and $[NiL](BF_4)\bullet H_2O$ **4** (red) **after** carrying out a controlled coulometry experiment as 1 $mmol.L^{-1}$ solutions in MeCN (200 $mV.s^{-1}$, 0.1 $mol.L^{-1}$ NEt_4PF_6, platinum electrode, versus 0.01 $mol.L^{-1}$ $AgNO_3$/Ag). All of these complexes show the emergence of a reversible redox process in close proximity to 0 V.

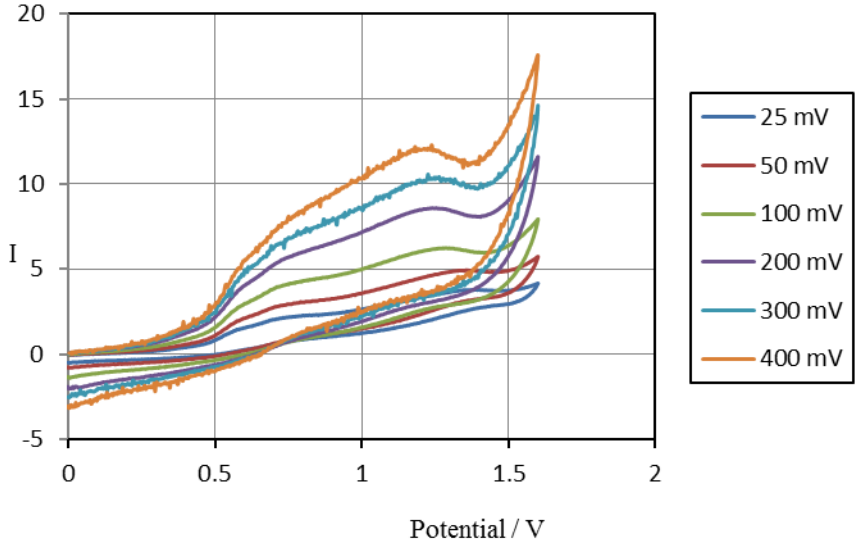

Figure S29. Cyclic voltammograms of $[Co^{II}L](BF_4)\bullet H_2O$ (oxidation process) at different scan rate ($mV.s^{-1}$).

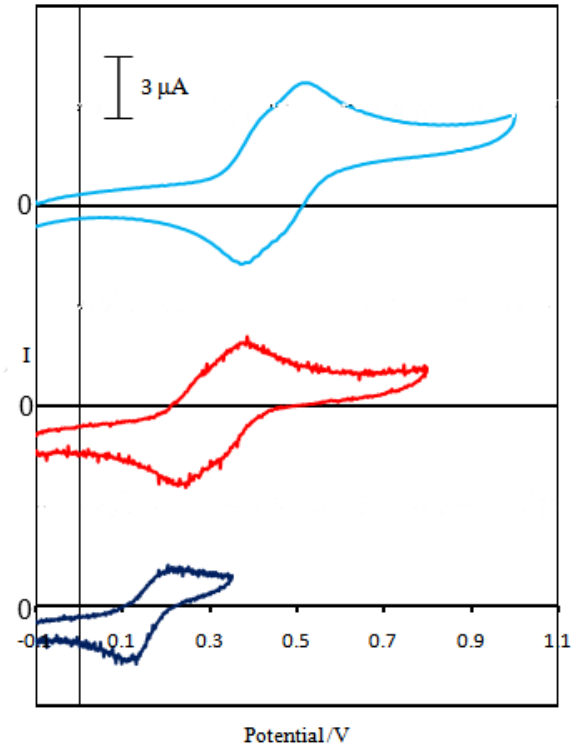

Figure S30. Cyclic voltammograms of complexes ***after*** a controlled potential coulometry experiment at the appropriate redox potential (Table 4), over the potential range of interest for, from bottom to top: $[Zn^{II}LPy](BF_4)$ **2** (blue line), $[Cu^{II}L](BF_4)\bullet H_2O$ **3** (red line) and $[Ni^{II}L](BF_4)\bullet H_2O$ **4** (pale blue line) as 1 $mmol.L^{-1}$ solutions in MeCN (200 $mV.s^{-1}$, 0.1 $mol.L^{-1}$ NBu_4PF_6, platinum electrode, versus 0.01 $mol.L^{-1}$ $AgNO_3/Ag$).

Table S1. Scan rate study of the process at approximately +0.37 V, for [ZnL(py)](BF_4), from 0 to +0.37 to 0 V, **before** conducting a controlled coulometry experiment.

	Epc	Epa	ΔE
25	+0.32	+0.30	0.02
50	+0.35	+0.31	0.04
100	+0.36	+0.31	0.05
200	+0.37	+0.32	0.05
300	+0.38	+0.32	0.06
400	+0.39	+0.33	0.06

Table S2. Scan rate study of the process at approximately +0.82 V, for [ZnL(py)](BF_4)), from 0 to +0.82 to 0 V, **before** conducting a controlled coulometry experiment.

	Epc	Epa	ΔE
25	+0.79	+0.79	0.00
50	+0.80	+0.78	0.02
100	+0.81	+0.78	0.03
200	+0.82	+0.77	0.05
300	+0.83	+0.78	0.05
400	+0.85	+0.78	0.07

Table S3. Scan rate study of the process at approximately +0.18 V, for [ZnL(py)](BF_4), from 0 to +0.18 to 0 V, **after** conducting a controlled coulometry experiment at +0.48 V which transferred 1.2 é equivalents per complex.

	Epc	Epa	ΔE
25	+0.18	+0.13	0.05
50	+0.19	+0.13	0.06
100	+0.20	+0.13	0.07
200	+0.20	+0.12	0.08
300	+0.21	+0.11	0.10
400	+0.21	+0.11	0.10

Table S4. Scan rate study of the process at approximately +0.50 V, for [CuL)](BF_4)•H_2O, from 0 to +0.50 to 0 V, **before** conducting a controlled coulometry experiment.

	Epc	Epa	ΔE
25	+0.50	+0.44	0.06
50	+0.50	+0.44	0.06
100	+0.51	+0.45	0.06
200	+0.50	+0.45	0.05
300	+0.50	+0.44	0.06
400	+0.50	+0.44	0.06

Table S5. Scan rate study of the process at approximately +0.36 V, for [CuL)](BF$_4$)•H$_2$O, from 0 to +0.36 to 0 V, **after** conducting a controlled coulometry experiment at +0.61 V which transferred 1 é equivalents per complex.

	Epc	Epa	ΔE
25	+0.36	+0.25	0.11
50	+0.36	+0.25	0.11
100	+0.37	+0.24	0.13
200	+0.37	+0.24	0.13
300	+0.38	+0.24	0.14
400	+0.39	+0.23	0.16

Table S6. Scan rate study of the process at approximately +0.59 V, for [NiL)](BF$_4$)•H$_2$O, from 0 to +0.59 to 0 V, **before** conducting a controlled coulometry experiment.

	Epc	Epa	ΔE
25	+0.59	+0.54	0.05
50	+0.58	+0.54	0.04
100	+0.58	+0.54	0.04
200	+0.59	+0.54	0.05
300	+0.59	+0.53	0.05
400	+0.59	+0.53	0.06

Table S7. Scan rate study of the process at approximately +1.37 V, for [NiL)](BF$_4$)•H$_2$O, from 0 to +1.37 to 0 V, **before** conducting a controlled coulometry experiment.

	Epc	Epa	ΔE
25	+1.30	+1.28	0.02
50	+1.32	+1.30	0.02
100	+1.33	+1.30	0.03
200	+1.37	+1.30	0.07
300	+1.36	+1.25	0.11
400	+1.35	+1.23	0.12

Table S8. Scan rate study of the process at approximately +0.48 V, for [NiL)](BF$_4$)•H$_2$O, from 0 to +0.50 to 0 V, **after** conducting a controlled coulometry experiment at +0.71 V which transferred 1.6 é equivalents per complex.

	Epc	Epa	ΔE
25	+0.50	+0.39	0.11
50	+0.50	+0.38	0.12
100	+0.50	+0.38	0.12
200	+0.50	+0.39	0.11
300	+0.50	+0.38	0.12
400	+0.50	+0.38	0.12

Table S9. Summary and comparison of the frequency and structural features of combinations of different chelate ring sizes in 4-coordinate Cu^{II} and Ni^{II} complexes and 6-coordinate Fe^{III} complexes of 12- to 16-membered N_4 macrocycles. Data obtained from searches of the CSD (version 5.31), analysed by Vista.

Complex	6666	6665	6655	6565	6555	5555
Any 3d	All-2283	All- 272	All-104	All-1871	All-79	All-310
	Cu-160	Cu-42	Cu-3	Cu-132	Cu-5	Cu
	Ni-355	Ni-37	Ni-15	Ni-292	Ni-12	Ni-6
	Fe-321	Fe-1	Fe-3	Fe-65	Fe	Fe-16
Any 3d NOT porphyrin/corrin	All-183	All-150	All-104	All-1827	All-78	All-308
	Cu-13	Cu-2	Cu-3	Cu-77	Cu-1	Cu-0
	Ni-23	Ni-8	Ni-15	Ni-162	Ni-5	Ni-2
	Fe-0	Fe-0	Fe-1	Fe-4	Fe-0	Fe-0
M-N(66) range (average) [Å]	Cu 1.93-2.08 (1.99)	Cu 1.92-2.06 (1.95)	Cu 1.93-1.97 (1.95)			
	Ni 1.85-1.97 (1.89)	Ni 1.88-1.98 (1.91)	Ni 1.93-2.00 (1.97)			
	Fe-none	Fe-none	Fe-2.15			
M-N(65) range (average) [Å]		Cu 1.91-2.06 (1.96)	Cu 1.99-2.05 (2.03)	Cu 1.86-2.16 (1.98)	Cu 1.81-2.01 (1.95)	
		Ni 1.85-1.99 (1.90)	Ni 1.86-1.99 (1.92)	Ni 1.80-2.10 (1.94)	Ni 1.85-1.90 (1.88)	
		Fe-none	Fe 2.11-2.15 (2.14)	Fe 1.95-2.03 (1.97)	Fe-none	
M-N(55) range (average) [Å]			Cu 1.88-1.92 (1.90)		Cu 1.84-1.99 (1.92)	Cu-none
			Ni 1.82-1.90 (1.85)		Ni 1.86-2.01 (1.92)	Ni 1.87-1.94 (1.89)
			Fe 2.11		Fe-none	Fe-none
***Cis* N-M-N range within 66, 65 and 55 chelate rings(average) [°]**	Cu 83.95-98.66 (90.48)	Cu 85.95-100.67 (92.73)	Cu 98.14-99.68 (98.78)	Cu 87.76-103.18 (95.38)	Cu 86.18-89.47 (86.95)	
	Ni 86.98-93.78 (90.06)	Ni 89.57-93.75 (91.74)	Ni 93.66-98.50 (96.36)	Ni 87.85-97.81 (93.46)	Ni 86.67-90.52 (89.19)	
	Fe-none	Fe-none	Fe-89.95	Fe-90.42-99.51 (94.31)	Fe-none	
***Cis* N-M-N range within 66, 65 and 55 chelate rings (average) [°]**		Cu 81.25-87.76 (85.28)	Cu 79.40-82.72 (81.21)	Cu 75.82-92.23 (85.12)	Cu 88.95-93.57 (90.83)	Cu-none
		Ni 82.73-89.89 (89.46)	Ni 80.37-86.60 (83.49)	Ni 82.05-90.65 (86.33)	Ni 86.40-93.36 (90.23)	Ni 86.74-91.60 (89.34)
		Fe-none	Fe-77.26	Fe-80.49-88.07 (84.77)	Fe-none	Fe-none
***Trans* N1-M-N4 range (average) [°]**	Cu 146.61-178.40 (170.77)	Cu 160.03-165.15 (163.49)	Cu 157.31-162.89 (160.18)	Cu 150.06-180.00 (176.18)	169.79	Cu-none
	Ni 155.84-179.46 (174.69)	Ni 163.42-172.99 (170.11)	Ni 171.49-179.52 (176.31)	Ni 160.45-180.00 (177.15)	Ni 167.16-176.84 (173.14)	Ni 161.83-170.77 (167.79)
	Fe-none	Fe-none	Fe 154.49	Fe 97-180 (166)	Fe-none	Fe-none
***Trans* N3-M-N2 range (average) [°]**	Cu 135.02-178.32 (168.42)	Cu 160.03-172.09 (169.07)	Cu 170.45-179.27 (175.77)	Cu 155.68-180.00 (175.97)	Cu-169.79	Cu-none
	Ni 163.62-179.46 (174.90)	Ni 162.90-172.99 (167.96)	Ni 161.25-169.45 (163.58)	Ni 162.40-180.00 (176.90)	Ni 165.94-176.84 (172.18)	Ni 162.98-167.37 (165.91)
	Fe-none	Fe-none	Fe 87.11	Fe 172.39-180 (179)	Fe-none	Fe-none

Figure S31. Summary of the *cis* (in diagram) and *trans* (in table) angles within different chelate ring sizes in 4-coordinate Cu^{II} complexes of 12- to 16- membered N_4 macrocycles. Data obtained from searches, with all bonds as any bond type, of the CSD (version 5.31), analyzed by Vista.

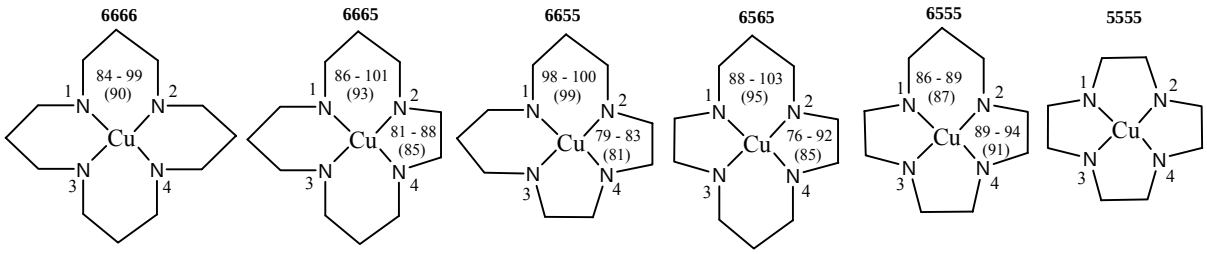

Hits	13	2	3	77	1	0
N1-Cu-N4 (average) [°]	147 – 178* (171)	160 – 165 (163)	157 – 163 (160)	150 – 180 (176)	169.79	
N3-Cu-N2 (average) [°]	135 – 178* (168)	160 – 173 (169)	170 – 179 (176)	155 – 180 (176)	169.79	

*A few them are outliers due to the buckled nature of the structures.

Figure S32. Summary of the *cis* (in diagram) and *trans* (in table) angles within different chelate ring sizes in 4-coordinate Ni^{II} complexes of 12- to 16- membered N_4 macrocycles. Data obtained from searches, with all bonds as any bond type, of the CSD (version 5.31), analyzed by Vista.

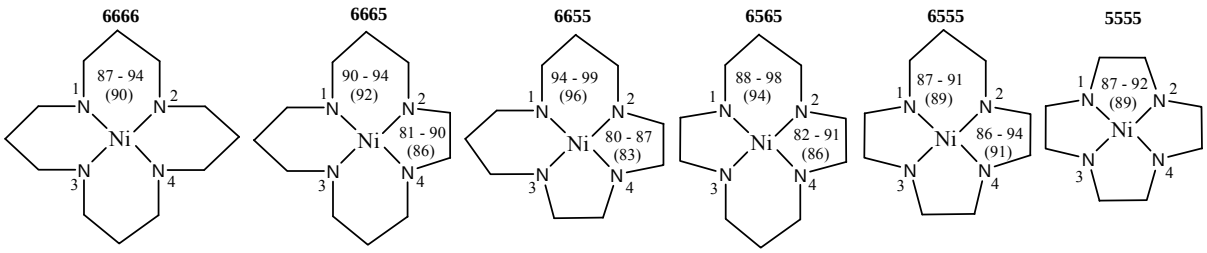

Hits	23	8	15	162	5	2
N1-Ni-N4 (average) [°]	156 – 180* (175)	163 – 173 (170)	171 – 180 (176)	160 – 180 (177)	167 – 177 (173)	162 – 171 (168)
N3-Ni-N2 (average) [°]	164 – 179 (175)	162 – 173 (168)	161 – 169 (164)	162 – 180 (177)	166 – 177 (172)	163 – 167 (166)

*A few them are outliers due to the buckled nature of the structures.

Figure S33. Summary of the *cis* and *trans* angles within different chelate ring sizes in 6-coordinate Fe^{III} complexes of 12- to 16- membered N_4 macrocycles. Data obtained from searches, with all bonds as any bond type, of the CSD (version 5.31), analyzed by Vista.

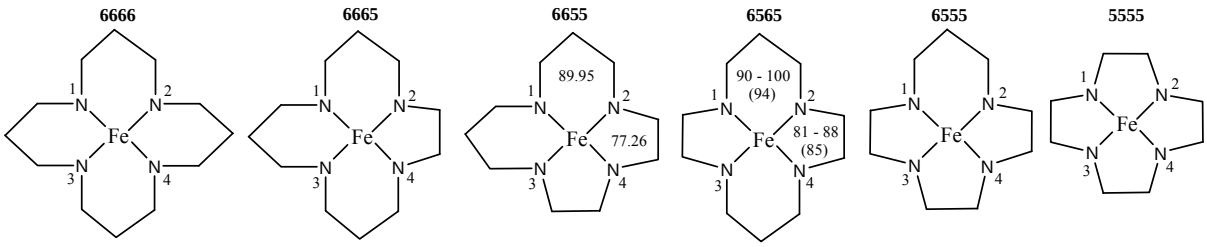

Hits	0	0	1	4	0	0
N1-Fe-N4 (average) [°]			154.49 °	97 – 180 (166)		
N3-Fe-N2 (average) [°]			87.11 °	172 – 180 (179)		

Figure S34. Summary of the bond lengths of different chelate ring sizes in 4-coordinate Cu^{II} complexes of 12- to 16- membered N_4 macrocycles. Data obtained from searches as any bond type of the CSD (version 5.31) and analyzed by Vista.

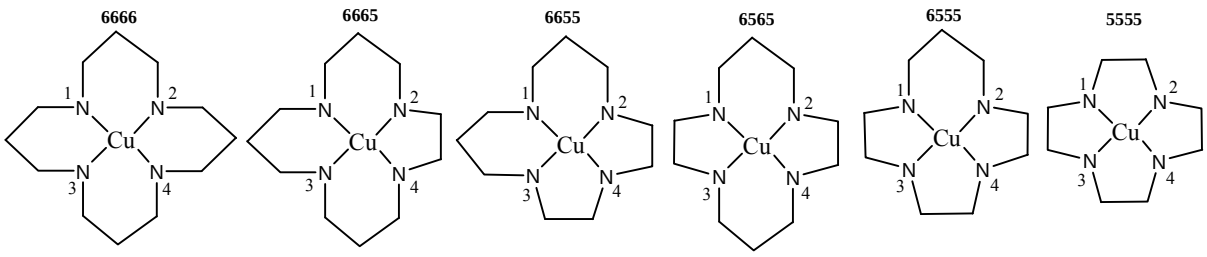

Hits	13	2	3	77	1	0
Cu-N 66 [Å]	1.93 – 2.08 (1.99)	1.92 – 2.06 (1.95)	1.93 – 1.97 (1.95)			
Cu-N 65 [Å]		1.91 – 2.06 (1.96)	1.99 – 2.05 (2.03)	1.86 – 2.16 (1.98)	1.81 – 2.01 (1.95)	
Cu-N 55 [Å]			1.88 – 1.92 (1.90)		1.84 – 1.99 (1.92)	

Figure S35. Summary of the bond lengths of different chelate ring sizes in 4-coordinate Ni^{II} complexes of 12- to 16- membered N_4 macrocycles. Data obtained from searches as any bond type of the CSD (version 5.31) and analyzed by Vista.

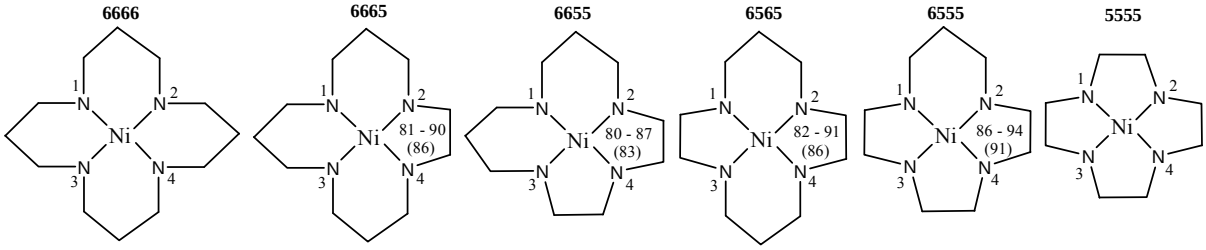

Hits	23	8	15	162	5	2
Ni-N 66 [Å]	1.85 – 1.97 (1.89)	1.88 – 1.98 (1.91)	1.93 – 2.00 (1.97)			
Ni-N 65 [Å]		1.85 – 1.99 (1.90)	1.86 – 1.99 (1.92)	1.80 – 2.10 (1.94)	1.85 – 1.90 (1.88)	
Ni-N 55 [Å]			1.82 – 1.90 (1.85)		1.86 – 2.01 (1.92)	1.87 – 1.94 (1.89)

Figure S36. Summary of the bond lengths of different chelate ring sizes in 6-coordinate Fe^{III} complexes of 12- to 16- membered N_4 macrocycles. Data obtained from searches as any bond type of the CSD (version 5.31) and analyzed by Vista.

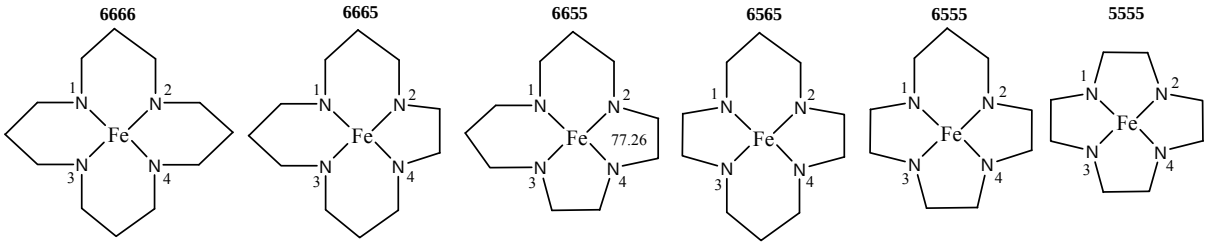

Hits	0	0	1	4	0	0
Fe-N 66 [Å]			2.15			
Fe-N 65 [Å]			2.11 – 2.15 (2.14)	1.95 – 2.03 (1.97)		
Fe-N 55 [Å]			2.11			

Table S10 Structures of all 4-coordinate Ni^{II} complexes of N_4 macrocycles with 6655 chelate rings in the CSD. See the following page for the general structure of these complexes (including R groups).

CCDC Codes for 4-coordinate Ni^{II}	R groups/Structure	Counter ion	References in paper
CEQVEA	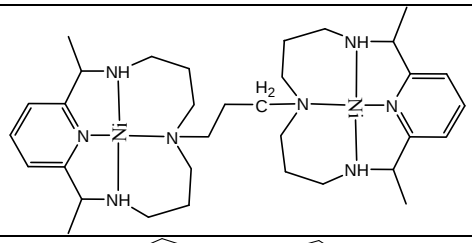	I	1
DOCDUU	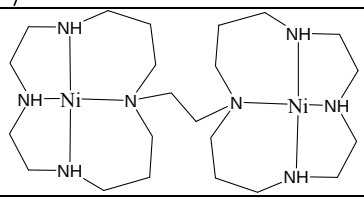	ClO_4	2
DOCVEW	$R_1 = H$ $R_2 = R_3 = CH_3$	ClO_4	3
DOGCOR	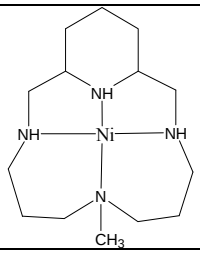	ClO_4	4
EFAHOJ	$R_1 = R_2 = R_3 = H$	ClO_4	5
FEJMOW	$R_1 = H$ $R_2 = R_3 = CH_3$	ClO_4	6
GEWPUT	$R_1 = R_2 = R_3 = CH_3$	ClO_4	7
IBOKUG	$R_1 = R_2 = H$ R3 = 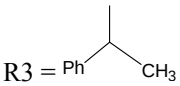	BF_4	8
MAZNIP	$R_1 = CH_3$ $R_2 = H$ $R_3 = H$	ClO_4	9
OGIRIG	$R_1 = CH3$ $R_2 = H$ R3 = 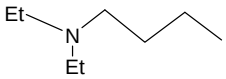	ClO_4	10
OGIROM	$R_1 = CH_3$ $R_2 = H$ R_3 = 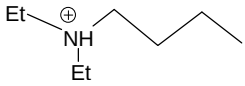	ClO_4	10
OGIRUS	$R_1 = CH_3$ $R_2 = H$ R_3 = 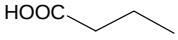	ClO_4	10
REDYII	$R_1 = R_2 = H$ $R_3 = CH_3$	ClO_4	11
TUWQUX	$R_1 = R_2 = H$ R3 = 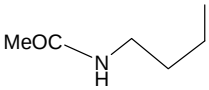	ClO_4	12

VAYGAD	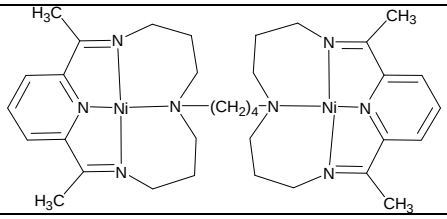	ClO_4	13

General structure of the dication in all of the above 4-coordinate Ni^{II} complexes (bonds "any type"):

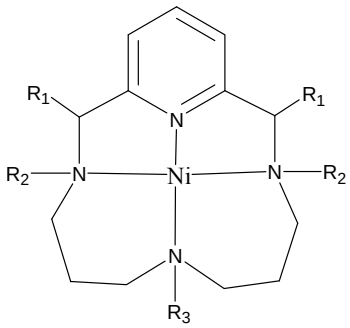

Table S11 Structures of all 4-coordinate Cu^{II} complexes of N_4 macrocycles with 6655 chelate rings in the CSD.

CCDC Codes for 4-coordinate Cu^{II}	**Structure**	**Counter ion**	**References in the paper**
INABOO	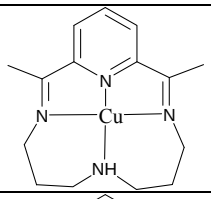	ClO_4	14
INABUU	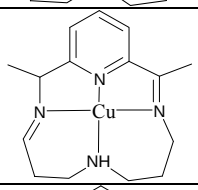	ClO_4	14
REDYEE	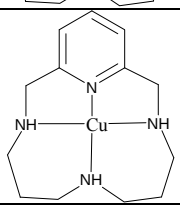	PF_6	11

Table S12 Structure of the only 6-coordinate Fe^{III} complex of an N_4 macrocycle with 6655 chelate rings in the CSD.

CCDC Code for 6-coordinate Fe^{III}	**Structure**	**Coordinated ion**	**Counter ion**	**Reference in the paper**
FOLDIT	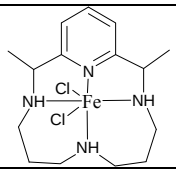	Cl	BF_4	15

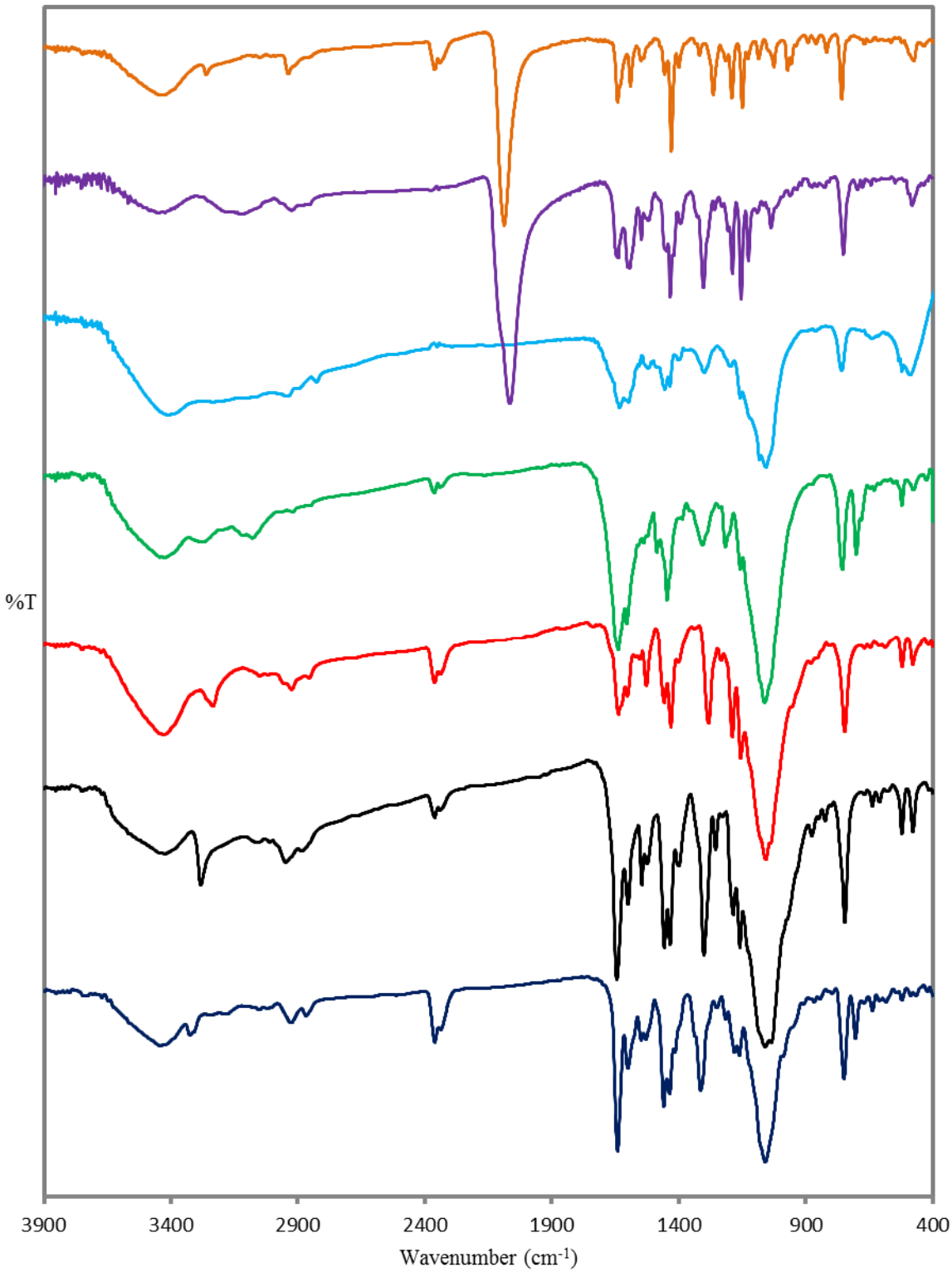

Figure S37. Infrared Spectra (KBr disks) from bottom to top: $[Zn^{II}L(py)](BF_4)$ **2** (navy blue line), $[Cu^{II}L](BF_4)\bullet H_2O$ **3** (black line), $[Ni^{II}L](BF_4)\bullet H_2O$ **4** (red line), $[Co^{II}L](BF_4)\bullet H_2O$ **5** (green line), $Fe^{III}L(BF_4)_2\bullet 2H_2O\bullet MeCN$ **6** (blue line), $[Co^{III}L(NCS)_2]\bullet 0.3py$ **7** (purple line), $[Fe^{III}L(NCS)_2]$ **8** (orange line).

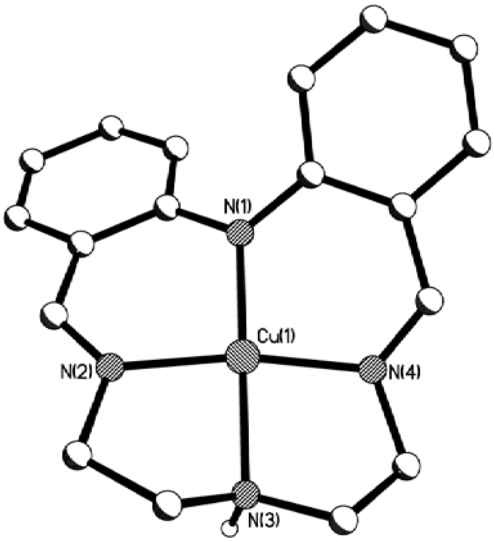

Figure S38. Perspective view of the cation of $[Cu^{II}L](BF_4)$. Hydrogen atoms and tetrafluoroborate anion omitted for clarity.

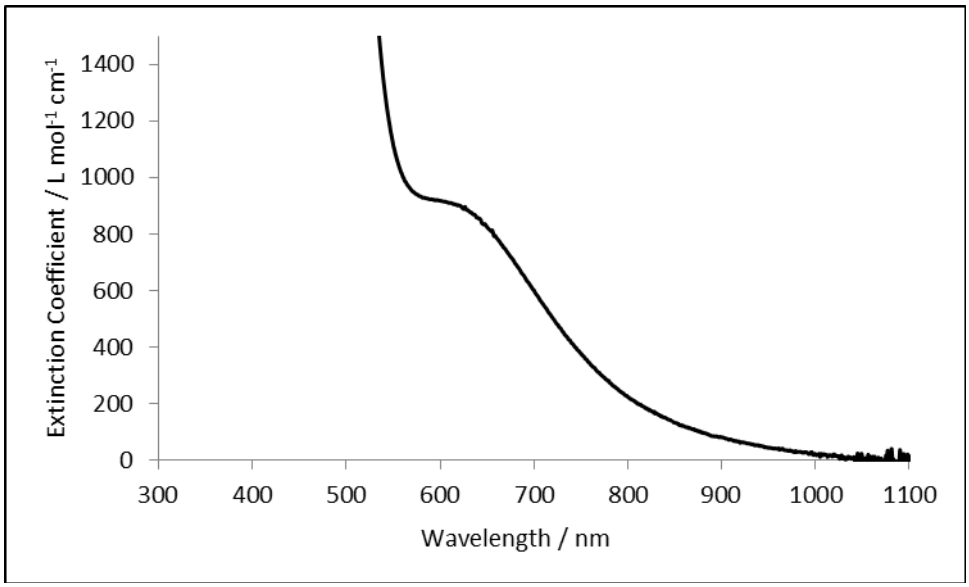

Figure S39. UV-vis spectrum of $[Co^{II}L](BF_4)\bullet H_2O$ **5** in MeCN, scaled so as to highlight the intense band tailing across the visible.

Table S13 Crystal structure determination details for the complexes 2{[ZnL(py)](BF$_4$)}•py, [NiL](BF$_4$), [CuL](BF$_4$), and [FeL(NCS)$_2$]•NO$_2$Me

	2{[Zn^{II}LPy](BF$_4$)}•py	[Cu^{II}L](BF$_4$)	[Ni^{II}L](BF$_4$)	[Fe^{III}L(NCS)$_2$]•NO$_2$Me
Emprical formula	$C_{51}H_{53}N_{11}B_2F_8Zn_2$	$C_{18}H_{19}N_4$ BF_4Cu	$C_{18}H_{19}N_4$ BF_4Ni	$C_{21}H_{22}N_7$ O_2S_2Fe
M_r	1124.40	441.72	436.89	524.43
Crystal system	Triclinic	Monoclinic	Monoclinic	Orthorhombic
Space group	P1 (twinned)	P2$_1$/n (twinned)	Pn	P2$_1$2$_1$2$_1$
a [Å]	10.3702(16)	12.058(3)	7.2737(15)	8.894(8)
b [Å]	10.6201(18)	7.4261(18)	10.6471(18)	13.097(12)
c [Å]	12.6948(19)	19.403(4)	11.3778(15)	19.980(15)
α [°]	96.434(8)	90	90	90
β [°]	98.583(8)	94.651(15)	94.181(3)	90
γ [°]	116.065(7)	90	90	90
V [Å^3]	1216.8(3)	1731.6(7)	878.8(3)	2327(3)
Z	1	4	2	4
T [K]	90(2)	90(2)	90(2)	90(2)
$\rho_{calcd.}$ [gcm^{-3}]	1.534	1.694	1.651	1.497
μ [mm^{-1}]	1.067	1.314	1.156	0.861
F(000)	578	900	448	1084
Crystal size [mm]	0.20 x 0.20 x 0.04	0.30 x 0.08 x 0.08	0.20 x 0.10 x 0.08	0.27 x 0.12 x 0.11
Θ range for data collection [°]	2.18 to 26.55	1.92 to 25.50	1.79 to 26.02	3.07 to 25.34
Reflections collected	19349	4205	11732	19217
Independent reflections	9848	4318	3339	4241
R(int)	0.0595	0.0000	0.0574	0.1131
Max. and min. transmission	0.9586 and 0.8150	0.9021 and 0.6939	0.9132 and 0.6614	0.9112 and 0.5840
Data/ restraints/ parameters	9848 / 3 / 650	4318 / 0 / 254	3339 / 2 / 257	4241 / 0 / 299
Goof (F^2)	1.040	1.180	1.014	1.038
R$_1$ [I > 2σ(I)]	0.0819	0.0767	0.0504	0.0652
wR$_2$ [all data]	0.2265	0.2081	0.1169	0.1484